Volcanic and impact deposits of the Moon's Aristarchus Plateau: A new view from Earth-based radar images

Bruce A. Campbell
Lynn M. Carter
Center for Earth and Planetary Studies, Smithsonian Institution, MRC 315, Washington D.C. 20013-7012, USA
B. Ray Hawke
Hawai'i Institute of Geophysics and Planetology, University of Hawai'i, 1680 East-West Road, Honolulu, Hawai'i 96822, USA
Donald B. Campbell
Department of Astronomy, Cornell University, Ithaca, New York 14853, USA
Rebecca R. Ghent
Department of Geology, University of Toronto, Earth Sciences Centre, 22 Russell Street, Toronto, Ontario M5S 3B1, Canada

ABSTRACT

Lunar pyroclastic deposits reflect an explosive stage of the basaltic volcanism that filled impact basins across the nearside. These fine-grained mantling layers are of interest for their association with early mare volcanic processes, and as possible sources of volatiles and other species for lunar outposts. We present Earth-based radar images, at 12.6 and 70 cm wavelengths, of the pyroclastic deposit that blankets the Aristarchus Plateau. The 70 cm data reveal the outlines of a lava-flow complex that covers a significant portion of the plateau and appears to have formed by spillover of magma from the large sinuous rille Vallis Schröteri. The pyroclastics mantling these flows are heavily contaminated with rocks 10 cm and larger in diameter. The 12.6 cm data confirm that other areas are mantled by 20 m or less of material, and that there are numerous patches of 2 cm and larger rocks associated with ejecta from Aristarchus crater. Some of the radar-detected rocky debris is within the mantling material and is not evident in visible-wavelength images. The radar data identify thick, rock-poor areas of the pyroclastic deposit best suited for resource exploitation.

Keywords: radar, moon, volcanism, cratering, impact deposits, pyroclastic.

INTRODUCTION

Lunar pyroclastic deposits are blankets of fine-grained glass and quenched-crystal spheroids formed by eruptions of gas-rich magma during the early phases of the basaltic volcanism that flooded most basin floors (Head, 1974; Wilson and Head, 1981). They are typically rich in iron oxides, and contain widely varying amounts of the mineral ilmenite, $FeTiO_3$. The distribution, composition, and glass fraction of the pyroclastics offer clues to the opening stages of lunar volcanism, and are often studied through optical and/or infrared remote sensing (e.g., McEwen et al., 1994; Weitz et al., 1998). Imaging radar observations provide complementary information on the physical properties of the mantling layers associated with volcanic processes and subsequent impact modification (Zisk et al., 1977; Gaddis et al., 1985).

The spheres trap solar wind hydrogen, ^{3}He, and carbon, and species such as sulfur and zinc occur as sublimate coatings. Studies of returned samples, such as the pyroclastic spheres found at the Apollo 17 site (Arndt and von Engelhart, 1987), suggest that simple processing (Allen et al., 1996) can extract components that may be significant resources for a lunar base (e.g., Wittenberg et al., 1987; Hawke et al., 1990). Because the deposits comprise submillimeter spheres, excavation will be less difficult than in the rocky regolith on mare lava flows (Horz et al., 1991). A major question for resource planning is the degree to which the pyroclastic deposits are contaminated by blocky debris hurled from distant impact craters, excavated from the underlying terrain, or formed in place by welding during the eruption, that might hamper processing and reduce the recovery fraction of important components.

This study addresses the largest lunar pyroclastic deposit, which mantles the Aristarchus Plateau, using Earth-based radar images at wavelengths that characterize centimeter- to decimeter-scale rock abundance over a range of depths within the target material. These data offer a new window on the physical properties of the near-surface deposits, the interplay of volatile-rich eruptions and flood-like lavas, and the subsequent changes in rock abundance caused by large and small impact craters across the plateau.

REGIONAL SETTING

The Aristarchus Plateau (Fig. 1) is a block of ancient highland crust, 170 km by 200 km, that rises 2 km above the surrounding basaltic plains (maria). This block was uplifted during formation of the Imbrium basin ~3.85 b.y. ago (Wilhelms, 1987). Subsequent bombardment created numerous craters, to ~55 km in diameter, and a several-meters-thick regolith. After a few hundred million years, eruptions covered the plateau with a mixture of basalt flows and fine-grained pyroclastics. The pyroclastics appear to be almost entirely composed of glass spheroids (Lucey et al., 1986; Weitz et al., 1998) with low titanium content (Wilcox et al., 2006). Deposit thickness is estimated to be 20–30 m from studies of partially filled craters (Zisk et al., 1977; McEwen et al., 1994), but local variations are not well characterized. Additional magma was erupted rapidly, forming sinuous rilles by a combination of thermal and mechanical erosion and construction of cooled levees. Vallis Schröteri may also have formed, in part, by exploitation of preexisting tectonic structures (Zisk et al., 1977). Some of this magma flowed into Oceanus Procellarum to form smooth plains. The 40 km crater Aristarchus formed within the past few hundred million years, covering parts of the plateau with a layer of impact ejecta (Guest and Spudis, 1985; Weitz et al., 1998).

REMOTE SENSING DATA

In 2005–2006, we collected radar images of the Aristarchus region, at 12.6 cm (Fig. 2) and 70 cm (Fig. 3) wavelengths, using the Arecibo and Green Bank telescopes. The images are obtained by transmitting a circularly polarized signal and receiving both reflected circular polarization states (Campbell et al., 2007). Reflections that match the polarization expected from a mirror-like surface are termed opposite-sense circular (OC), and those with the orthogonal polarization state are termed same-sense circular (SC). The SC echoes arise from scattering by wavelength-scale blocks on and within the regolith, so they form the main element of this study.

The radar signals penetrate the dry regolith and are scattered back to the receiving antenna by subsurface rocks or rough interfaces. The maximum depth of probing is constrained by the microwave loss properties of the target material, but is typically 10–20 wavelengths. The loss properties are determined by the composition of the lunar material, with greater amounts of ilmenite, in particular, leading to greater attenuation of the incident signal (Carrier et al., 1991; Campbell et al., 1997). Radar studies show that lunar pyroclastics have very low backscatter due to their low volume rock abundance, and perhaps to greater microwave losses (Zisk et al., 1977; Gaddis et al., 1985). This is most evident along the southwestern flank of the Plateau, where the low 12.6 cm and 70 cm radar echoes (Figs. 2 and 3) contrast sharply with the higher echoes from the mare regolith.

The Clementine spacecraft collected images of the Moon in five color bands via the ultraviolet-visible (UV) camera and 6 infrared bands via the near-infrared (IR) camera. These data can be processed by band-ratio methods to reveal differences between mature glass-rich materials, fresh exposures of iron-rich mafic minerals, and fresh low-iron highlands material (McEwen et al., 1994; Weitz et al., 1998). Comparison of Clementine data with Apollo samples led to an empirical model for FeO abundance in lunar soils that better discriminates basaltic from feldspathic material (Fig. 4) (Lucey et al., 2000). An analogous technique for TiO_2 content is not used here due to uncertainties in its application to glass-rich materials, which were not included in the original model development. For similar reasons, we do not use the FeO map as a quantitative guide, but rather as a means to discriminate low-FeO materials excavated from a highlands basement against a background of higher-FeO materials that comprise some mixture of the pyroclastic glasses and excavated mare basalt.

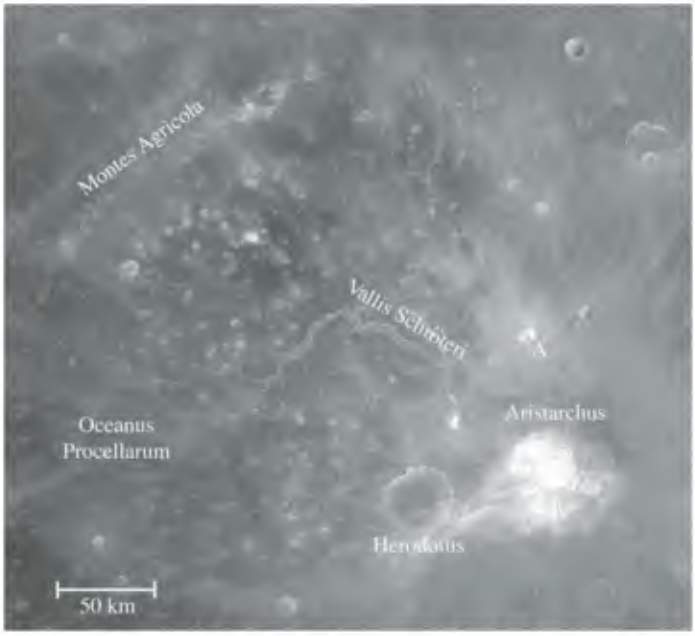

Figure 1. Reflectance image (750 nm) of the Aristarchus Plateau collected by Clementine spacecraft. Image resolution is ~150 m per pixel.

Figure 2. Earth-based radar image of Aristarchus Plateau at 12.6 cm wavelength (same-sense circular polarization). Spatial resolution of the base image is 25 m per pixel; averaged here to 150 m per pixel. Radar echoes are brighter in areas with abundant surface and near-surface rocks >~2 cm in diameter.

PLATEAU VOLCANIC HISTORY

The visible surface of the plateau is dominated by the pyroclastics, though some areas are covered by crater ejecta that mask the UV-visible–IR signatures of older deposits. Of interest for the volcanic history of

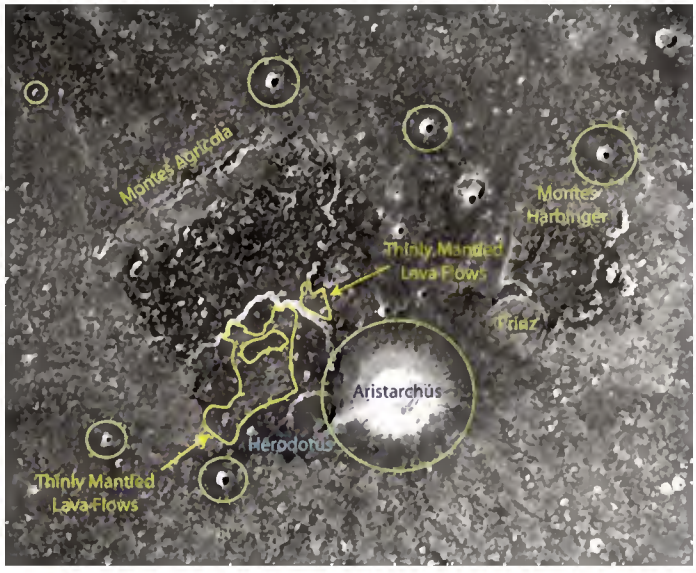

Figure 3. Earth-based radar image at 70 cm wavelength (same-sense circular polarization) of Aristarchus region. Low-radar-return areas of plateau are mantled by ≤20 m of pyroclastic glasses. Areas outlined in yellow have 70 cm radar echo strength comparable to nearby mare regions, but are mantled by pyroclastics. Higher echoes indicate that lava flows underlie the mantling debris. Green circles show extent of rock-poor ejecta haloes around younger impact craters.

this region is the extent of mare basalt coverage across the plateau. Fine-grained pyroclastics represent a small fraction of the erupted magma volume, so the large area covered and inferred thickness imply some combination of flow complexes beneath the mantling material and discharge of lava into the nearby lowlands (Weitz et al., 1998). The presence of basalt flows beneath the pyroclastic mantle was suggested by Zisk et al. (1977) for areas of the plateau that appear smooth at the kilometer scale; these flows were contemporaneous with the earliest pyroclastic eruptions, and thus mantled only by the latest of the fire-fountain materials. Analysis of Clementine data confirmed the presence of mare material in the walls of Vallis Schröteri and some small craters (McEwen et al., 1994).

Our 70 cm data reveal the outlines of an extensive basalt complex on the plateau, inferred from the boundaries of a higher-radar-return region (Fig. 3) that includes smooth areas previously mapped as mantled mare and some terrain mapped as "hummocky" by Zisk et al. (1977). The mare-floored area is covered by pyroclastics, but the 70 cm echoes are similar to those of mare deposits southwest of the plateau. The region of high 70 cm return extends to the rim of Vallis Schröteri in two locations, suggesting that the lava originated as spillover from the rille. While it is likely that Vallis Schröteri formed at least in part as a tectonic feature, with thermal and/or mechanical erosion forming the narrow channel in the valley floor, these spillovers suggest that the magma at least briefly filled the main channel.

A map of FeO abundance (Fig. 4) shows almost no small craters that excavate low-iron highland materials in the areas mapped by Zisk et al. (1977) as mantled basalt, in contrast to numerous such craters across the northwest portion of the plateau. Within the additional area of mantled basalt suggested by the radar data, there is a sparse population of small, low-FeO patches that may be craters or highland massifs. Hummocky outcrops are particularly evident where they follow the rim of a 55 km degraded impact crater.

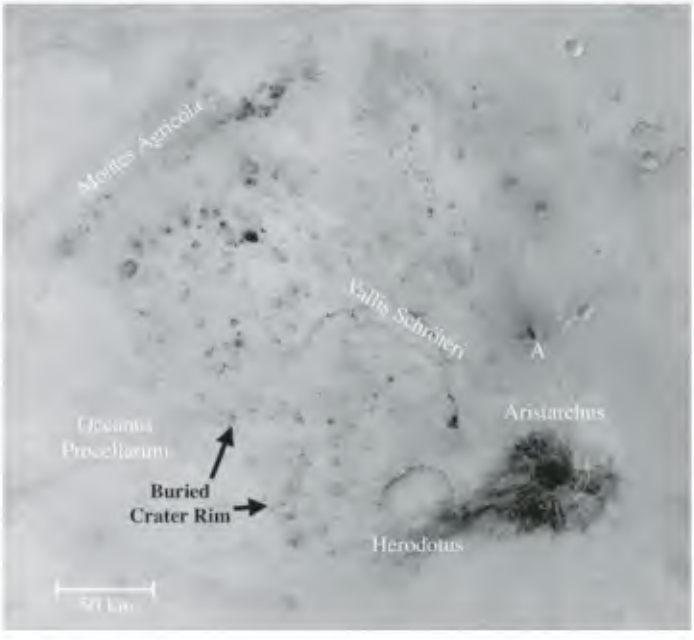

Figure 4. Map of the abundance of FeO in surface materials (Lucey et al., 2000). Areas with FeO content <8% shown as black, areas with FeO >21% shown as white. Brighter signatures are relatively homogeneous across the mare and plateau due to similar iron content of the basalt flows and pyroclastics. Low-iron patches correlate with highland outcrops and small craters that excavate the plateau materials below the volcanic deposits.

The thickness of the pyroclastics in the radar-dark parts of the plateau may be estimated from the smallest young craters that excavate rocky (radar bright) debris, and from the morphology of partially filled old craters (Zisk et al., 1977; McEwen et al., 1994). In the northwest and west parts of the plateau, ancient craters as small as 100 m in diameter, *D*, remain visible in Lunar Orbiter photos, though mostly filled by mantling material. Small crater depth is typically *D*/5 (Pike, 1980) so the pyroclastic layer is no more than ~20 m thick. Primary craters, which excavate blocky, radar-bright material from a maximum depth of *D*/10 (Pike, 1980), can be identified down to 200 m diameter in the 12.6 cm data, confirming that the mantle is <20 m thick.

The pyroclastic deposit is thinner above the lava complex, since these flows buried any earlier materials. Lunar Orbiter images of this area show more pronounced relief on craters 400–500 m in diameter that predate the volcanism on the plateau than on old craters of similar size in the radar-dark areas. Because 20 m is an upper estimate of thickness in the radar-dark regions, and part of the crater-filling deposits in the radar-bright region are lava flows, a reasonable estimate is that the pyroclastics are no more than ~10 m thick. Other areas mapped as mantled maria along the northeast and northwest margins of the plateau by Zisk et al. (1977) have lower 70 cm SC echoes, suggesting a thicker (i.e., 20 m) cover of pyroclastics.

The mantling deposit above the lava flows is heavily contaminated by debris from the underlying basalt, based on enhanced radar echoes and the presence of numerous radar-bright points that we infer to be rocky material excavated by craters that penetrate the mantle. The pyroclastics have low TiO_2 content, so their loss tangent may be at the low end of the range measured for lunar basaltic materials (Carrier et al., 1991), allowing a penetration depth of ~3 m at 12.6 cm wavelength and ~15 m at 70 cm wavelength. The higher 12.6 cm radar returns from these areas, which are almost as bright as mare deposits surrounding the plateau, suggest a large population of suspended rocks 2 cm and larger (Fig. 5). The 70 cm echoes, which are sensitive to rocks 10 cm and larger, are nearly as bright in this area as in mare deposits southwest of the plateau (Fig. 3). Since 70 cm signals may penetrate the deposit, the high echoes represent a combination of reflections from suspended rocks and from the buried lava flow surface.

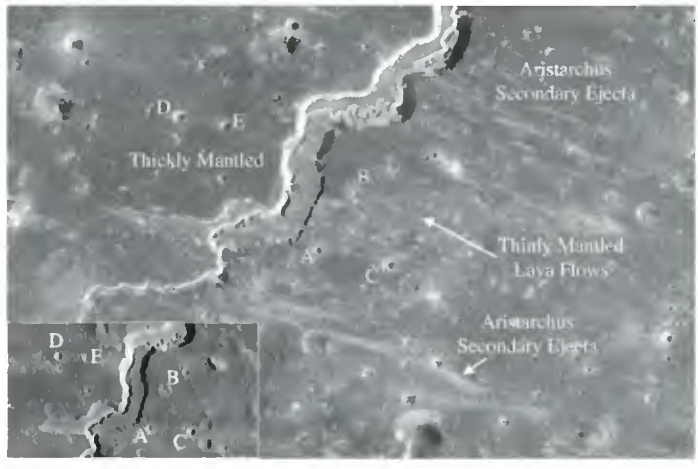

Figure 5. Radar image at 12.6 cm wavelength (25 m resolution) of the distal portion of Vallis Schröteri, where thick (radar-dark with few bright features) and thin (radar-bright areas with numerous small, bright craters and streaks) mantling materials flank the rille. Inset shows Lunar Orbiter IV photo, with small craters labeled (A–E) to match on both images. Note the lack of strong optical albedo features associated with the radar-bright secondary ejecta streaks across this area.

ROLE OF ARISTARCHUS CRATER EJECTA

The impact that formed Aristarchus contributes material to the near-surface layers on the plateau. There are numerous 12.6 cm radar-bright streaks (Fig. 2) radial to Aristarchus, and most appear to be secondary impacts of blocks from the main crater; a few are primary impacts that excavate rocky debris from beneath the mantling deposit. Radial features with high radar return are often associated with broad, faint increases in surface albedo, but some albedo contrasts around secondary craters have no distinct radar enhancement (Figs. 1, 2, and 5). We suggest that the radar senses deposits of rocks, with diameter greater than ~2 cm, formed by primary and secondary impacts. Some of these deposits are buried within the pyroclastic mantle. The albedo contrasts with no radar enhancement may be compositional differences between fine-grained materials that will fade as the regolith is overturned by small impacts.

Lunar craters have associated haloes of low 70 cm radar return (Ghent et al., 2005). These concentric deposits, noted in Figure 3, are relatively thick (more than several meters), rock-poor material produced during the excavation process. Aristarchus has a pronounced 70 cm halo where its ejecta overlie mare basalts south and east of the crater, and we expect that this halo extends onto the plateau. This means that surface layers near the head of Vallis Schröteri have an even greater depth of fine material, and a smaller component of resource-bearing glass beads, where the halo overlaps and incorporates the pyroclastics. It is interesting that neither radar map shows a strong difference in backscatter between the pyroclastic materials and ejecta distributed north and west of Aristarchus (Weitz et al., 1998). The low radar backscatter signature suggests that pyroclastic material is present across the area, covered by a veneer of rock-poor, mare-derived ejecta.

CONCLUSIONS

There is a marked dichotomy in the thickness and volume rock abundance of pyroclastic material on the Aristarchus Plateau. Much of the region south and east of Vallis Schröteri is underlain by a basalt flow complex, and mantled by perhaps 10 m of fine-grained glass with abundant rocky debris excavated by small impacts. Other areas on the plateau are mantled to a thickness of 20 m or less, but closer to Aristarchus this layer is thicker and more contaminated due to the addition of pulverized rock-poor debris that elsewhere forms the crater's radar-dark halo. Only north and west of Vallis Schröteri are the pyroclastics thick and free of large numbers of included rocks over areas a few kilometers or more in extent. The new radar data provide a window on the geologic history, resources, and potential hazards of this important region.

ACKNOWLEDGMENTS

Helpful reviews were provided by A. McEwen and W. Mendell. This work was supported by the National Aeronautics and Space Administration Planetary Astronomy and Planetary Geology and Geophysics Programs. Arecibo Observatory is part of the National Astronomy and Ionosphere Center, which is operated by Cornell University under a cooperative agreement with the National Science Foundation (NSF). The Green Bank Telescope is part of the National Radio Astronomy Observatory, a facility of the NSF operated under cooperative agreement by Associated Universities, Inc.

REFERENCES CITED

Allen, C.C., Morris, R.V., and McKay, D.S., 1996, Oxygen extraction from lunar soils and pyroclastic glasses: Journal of Geophysical Research, v. 101, p. 26,085–26,095, doi: 10.1029/96JE02726.

Arndt, J., and von Engelhardt, W. 1987, Formation of Apollo 17 orange and black glass beads: Journal of Geophysical Research, v. 92, p. E372–E376.

Campbell, B.A., Hawke, B.R., and Thompson, T.W., 1997, Long-wavelength radar studies of the lunar maria: Journal of Geophysical Research, v. 102, p. 19,307–19,320, doi: 10.1029/97JE00858.

Campbell, B.A., Campbell, D.B., Margot, J.L., Ghent, R.R., Nolan, M., Chandler, J., Carter, L.M., and Stacy, N.J.S., 2007, Focused 70-cm radar mapping of the Moon, 2007: Institute of Electrical and Electronics Engineers Transactions on Geoscience and Remote Sensing (in press).

Carrier, W.D., Olhoeft, G.R., and Mendell, W., 1991, Physical properties of the lunar surface, *in* Heiken, G.H., et al., eds., Lunar sourcebook: Cambridge, Cambridge University Press, p. 475–594.

Gaddis, L.R., Pieters, C.M., and Hawke, B.R., 1985, Remote sensing of lunar pyroclastic deposits: Icarus, v. 61, p. 461–489.

Ghent, R.R., Leverington, D.W., Campbell, B.A., Hawke, B.R., and Campbell, D.B., 2005, Earth-based observations of radar-dark crater haloes on the Moon: Implications for regolith properties: Journal of Geophysical Research, v. 110, E02005, doi: 10.1029/2004JE002366.

Guest, J.E., and Spudis, P.D., 1985, The Aristarchus impact event and the effects of target material: Geological Magazine, v. 122, p. 317–327.

Hawke, B.R., Coombs, C.R., and Clark, B., 1990, Ilmenite-rich pyroclastic deposits: An ideal lunar resource: Proceedings of the Lunar and Planetary Science Conference, 20th, p. 249–258.

Head, J.W., 1974, Lunar dark-mantle deposits: Possible clues to the distribution of early mare deposits: Proceedings of the Lunar and Planetary Science Conference, 5th, p. 207–222.

Horz, F., Grieve, R., Heiken, G., Spudis, P., and Binder, A., 1991, Lunar surface processes, *in* Heiken, G.H., et al., eds., Lunar sourcebook: Cambridge, Cambridge University Press, p. 61–120.

Lucey, P.G., Hawke, B.R., Pieters, C.M., Head, J.W., and McCord, T.B., 1986, A compositional study of the Aristarchus region of the Moon using near-infrared reflectance spectroscopy: Journal of Geophysical Research, v. 91, p. D344–D354.

Lucey, P.G., Blewett, D.T., and Joliff, B.D., 2000, Lunar iron and titanium abundance algorithms based on final processing of Clementine UV-visible images: Journal of Geophysical Research, v. 105, p. 20,297–20,306, doi: 10.1029/1999JE001117.

McEwen, A.S., Robinson, M.S., Eliason, E.M., Lucey, P.G., Duxbury, T.C., and Spudis, P.D., 1994, Clementine observations of the Aristarchus region of the Moon: Science, v. 266, p. 1858–1862, doi: 10.1126/science.266.5192.1858.

Pike, R.J., 1980, Geometric interpretation of lunar craters: U.S. Geological Survey Professional Paper 1046C, 77 p.

Weitz, C.M., Head, J.W., and Pieters, C.M., 1998, Lunar regional dark mantle deposits: Geologic, multispectral, and modeling studies: Journal of Geophysical Research, v. 103, p. 22,725–22,759, doi: 10.1029/98JE02027.

Wilcox, B.B., Lucey, P.G., and Hawke, B.R., 2006, Radiative transfer modeling of compositions of lunar pyroclastic deposits: Journal of Geophysical Research, v. 111, E09001, doi: 10.1029/2006JE002686.

Wilhelms, D.E., 1987, The geologic history of the Moon: U.S. Geological Survey Professional Paper 1348, 342 p.

Wilson, L., and Head, J.W., 1981, Ascent and eruption of basaltic magma on the Earth and Moon: Journal of Geophysical Research, v. 78, p. 2971–3001.

Wittenberg, L.J., Santarius, J.F., and Kulcinski, G.L., 1987, Lunar source of ^{3}He for commercial fusion power: Fusion Technology, v. 10, p. 167–178.

Zisk, S.H., Hodges, C.A., Moore, H.J., Shorthill, R.W., Thompson, T.W., Whitaker, E.A., and Wilhelms, D.E., 1977, The Aristarchus-Harbinger region of the Moon: Surface geology and history from recent remote-sensing observations: The Moon, v. 17, p. 59–99, doi: 10.1007/BF00566853.

Manuscript received 27 July 2007
Revised manuscript received 14 September 2007
Manuscript accepted 2 October 2007

Printed in USA